

Modeling Tritiated Water Desorption from Stainless Steel

Karin Hsieh

**Webster Schroeder High School
Rochester, NY**

Advisor: Dr. W. T. Shmayda

**Laboratory for Laser Energetics
University of Rochester
Rochester, NY
September 2010**

Abstract

A simple mathematical model has been developed to describe the outgassing rate of tritium from solids as a function of time. The model is based on the assumptions of a homogeneous material that can be characterized with a single diffusion coefficient. The model was used to fit the experimental tritium desorption rates from pre-tritiated, type 316, stainless steel over a temperature range of 20 to 400°C. The basic model did not fit the experimental data accurately at longer times, except for data obtained at 20 and 400°C. Including carrier gas flow rate and temperature ramping did not improve the fitting results at the longer times. It is likely that at 20°C, the desorption process is dominated by a single diffusion coefficient that describes tritium diffusion through and desorption from the surface oxide layer. At 400°C, the desorption process is dominated by atom transport through the bulk metal. At intermediate temperatures, atom transport is dependent on diffusivity through the oxide and the bulk, and thus resulted in a poor curve fit since the model assumes a unique diffusion coefficient within a single homogeneous layer. We conclude that the bulk diffusion model alone cannot describe the tritium desorption processes from stainless steel with an oxide top layer. A more accurate model that includes desorption from the surface oxide layer, diffusion through the oxide layer, and diffusion within the bulk has been proposed for future work.

Introduction

Tritium (H-3) is a radioactive, naturally occurring isotope of hydrogen, with a half-life of 12.32 years. Tritium has commercial, research, and defense applications. The commercial and research uses of tritium, which accounts for only a fraction of tritium used worldwide, include tracers in biological diagnostics and environmental studies and safety signs in low-light applications where electrical power is not available. Additionally, tritium provides an extremely sensitive tool for studying the fundamentals of water desorption from metals. A significant amount of research has gone into understanding how water bonds to and desorbs from surfaces. In particular, industries that require ultra-pure streams for their chemical processes (such as the semiconductor industry) have identified adsorbed water as a contaminant and work hard to eliminate water from the inside of metal process lines. Tritium-labeled water is an excellent tool for better understanding the processes.

The interest in the behavior of tritium in stainless steel mainly stems from its widespread usage in tritium-handling equipment and components. In addition to having excellent mechanical properties, stainless steel has favorable properties concerning hydrogen permeation and dissolution, hydrogen-induced embrittlement, and tritium-decay accelerated corrosion [1, 2]. A particular challenge to a systematic investigation of the interaction of hydrogen isotopes with stainless steel is the multi-elemental composition of the bulk, a different multi-element makeup in the near surface and a complex oxide structure. There is significant evidence in the literature describing the influence of the chemical composition of the surface on the kinetics of hydrogen absorption and desorption from stainless steel [1, 2].

Hydrogen and its isotopes behave similarly in many regards. They are diatomic gases that dissociate on metal surfaces and dissolve in the metal lattice as atoms. These atoms readily recombine once they return to any air-surface interface. This high mobility implies that metals in general are not good barrier materials for tritium [1, 2]. By contrast, ceramics and oxides are typically very good barrier materials if they are not porous. In most cases, the low permeation is due to extremely low solubility for hydrogen isotopes in ceramic materials, especially metal oxide materials [3, 4].

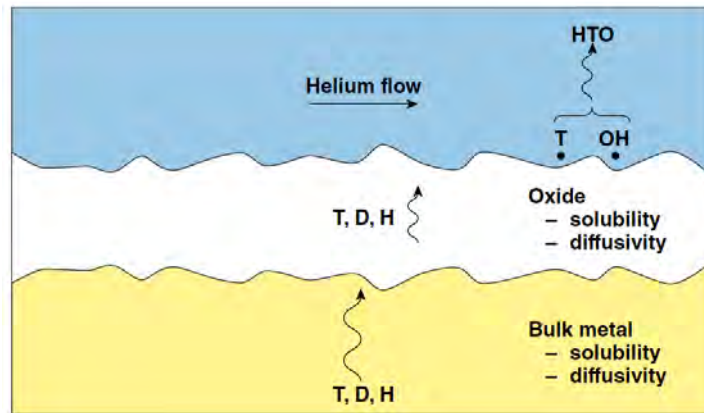


Fig. 1: Cross-section of a metal coupon in the vicinity of the metal-air interface

This paper describes the modeling of tritium transport from the bulk of 316, stainless steel to the surroundings in the presence of water vapor. The key aspects of the model are shown in Figure 1. Helium containing water vapor flows over the metal surface. Hydrogen isotopes diffuse from the bulk through the oxide layer and accumulate on the uppermost surface of the oxide. Water vapor collides with the surface and dissociates to form hydroxyl radicals and protons that remain bound to the surface. After residing on the surface for a short length of time that depends on the metal temperature among other factors, the protons and hydroxyl radicals recombine and desorb from the surface. Occasionally the hydroxyl radicals recombine with tritons instead of protons, which also reside on the surface to form tritiated water (HTO). In this case HTO desorbs from the surface. This desorption process depletes the concentration of tritons on the surface and establishes a concentration gradient between the surface and the bulk. Tritons migrate from the bulk to the surface as a result of the concentration gradient. A simple model based on diffusion from the bulk to the surface that uses a single diffusion constant is developed in a subsequent section and tested against experimental data. Understanding the factors that control tritium removal from metals is important if techniques to reduce chronic tritium emissions from metals are to be developed [4, 5].

Experimental Setup

The experimental setup to measure the rate of tritium release from contaminated coupons is provided in Figure 2.

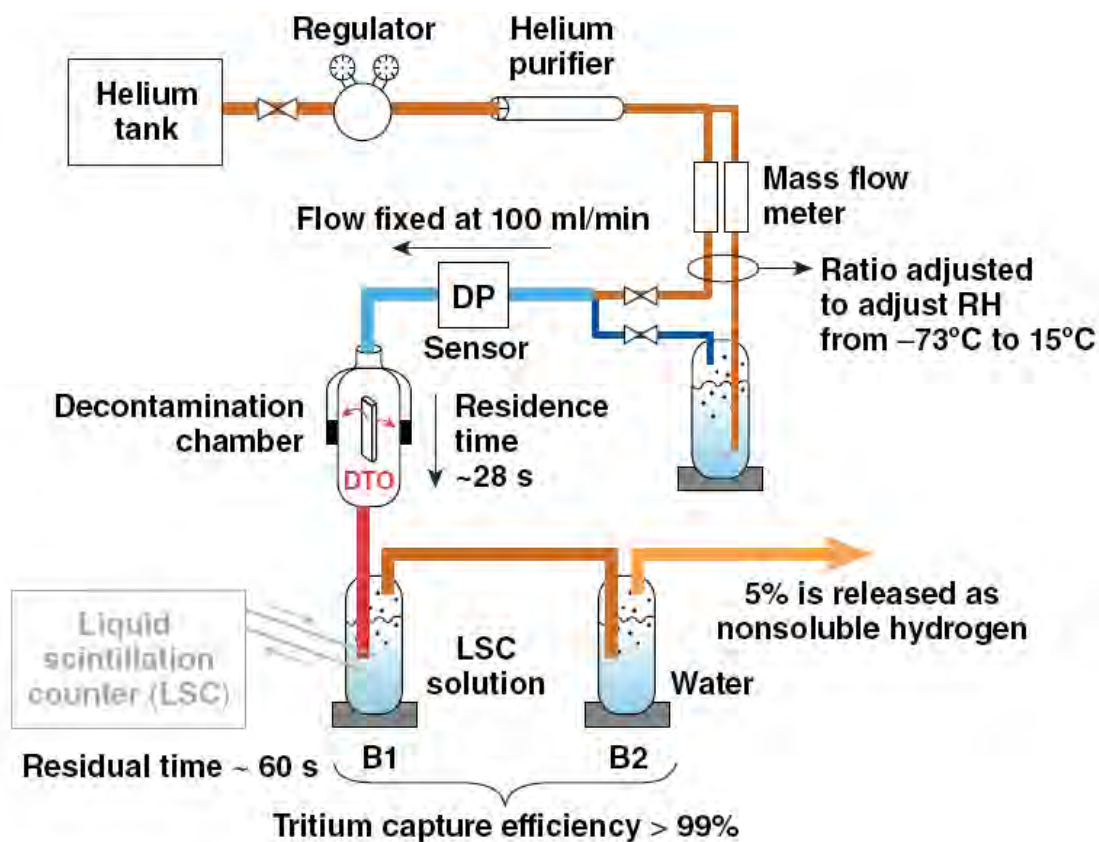


Fig. 2. Experimental setup to measure tritium desorption from contaminated coupons

Type 316, stainless steel coupons (5 x 1.8 x 0.3 cm) were contaminated by exposing them to 690 Torr of deuterium-tritium (DT) gas for 23 h at room temperature. Subsequently the coupons were stored in a dry helium environment and then transferred to the decontamination chamber under a helium blanket to ensure that air and humidity did not come in contact with the samples before the experiment. High purity helium was passed through a purifier to remove trace impurities and introduced into the decontamination chamber at 100 ml/min. The humidity of the helium carrier could be adjusted by diverting a fraction of the carrier through a wash bottle filled with water. The humidity was measured using a dew point sensor once the two streams were recombined before entering the decontamination chamber. In the current set of experiments the humidity of the carrier was held at -70°C or lower. At a flow rate of 100 ml/min, the gas content of the exposure chamber would be replaced every 28 seconds. Previous work has shown that more than 95% of the tritium that is released from a metal surface will be released as tritiated water (HTO) and more than 99% of the

tritium will be captured by a set of two bubblers [3,4]. The same contaminated coupon was used to investigate desorption at 25, 100, 150, 200, 250, 300, and 400°C respectively in this study.

Theory

Fick's second law of diffusion describes the concentration (c) of hydrogen in a metal as a function of time (t) and depth (x) [6].

$$\frac{\partial c}{\partial t} = D \frac{\partial^2 c}{\partial x^2}$$

The following boundary equations apply to hydrogen transport from the bulk of a metal sample of finite size to the surface:

$$\begin{aligned} c &= c_1, \text{ at } x = 0 \text{ for all times,} \\ c &= c_2, \text{ at } x = l \text{ for all times, and} \\ c &= c_0, \text{ at } t = 0 \text{ for } 0 < x < l \end{aligned}$$

The method of separation of variables is used to solve the above second order differential equation by assuming that the concentration comprises two parts, one dependent on position, the other on time:

$$c(x, t) = X(x)T(t)$$

Substituting into and reorganizing the diffusion equation to separate the variables, the diffusion equation becomes:

$$\frac{1}{T} \frac{dT}{dt} = \frac{d^2X}{dx^2} \left(\frac{D}{X} \right)$$

Since each side of this equation is independent of each other, they must equal the same constant, which is taken to be $-\lambda^2 D$.

$$\frac{1}{T} \frac{dT}{dt} = \frac{d^2X}{dx^2} \left(\frac{D}{X} \right) = -\lambda^2 D$$

The solutions for $T(t)$ and $X(x)$ are:

$$T(t) = e^{-\lambda^2 D t}$$

$$X(x) = A \sin(\lambda x) + B \cos(\lambda x)$$

where A and B are constants of integration. The concentration dependence on position and time, $c(x,t)$, can be written as:

$$c(x, t) = [A \sin(\lambda x) + B \cos(\lambda x)]e^{-\lambda^2 D t}$$

The general form of the above solution is the sum of solutions of the same type.

$$c(x, t) = \sum_{m=1}^{\infty} [A_m \sin(\lambda_m x) + B_m \cos(\lambda_m x)]e^{-\lambda_m^2 D t}$$

where the values of A_m , B_m , and λ_m are determined from the boundary and initial conditions listed above.

For $c = c_1$, at $x = 0$ to hold for all times, $B_m = 0$, and to satisfy the condition $c = c_2$ at $x = l$ for all times requires:

$$\lambda_m = \frac{m\pi}{l}$$

The concentration $c(x,t)$ reduces to:

$$c(x, t) = \sum_{m=1}^{\infty} \left[A_m \sin\left(\frac{m\pi x}{l}\right) \right] e^{-\frac{m^2 \pi^2 D}{l^2} t}$$

To meet the initial condition $c = c_0$, at $t = 0$ for $0 < x < l$ requires:

$$c(x, 0) = C_0 = \sum_{m=1}^{\infty} A_m \sin\left(\frac{m\pi x}{l}\right)$$

$$\int_0^l C_0 \sin\left(\frac{p\pi x}{l}\right) dx = \int_0^l \sum_{m=1}^{\infty} A_m \sin\left(\frac{m\pi x}{l}\right) \sin\left(\frac{p\pi x}{l}\right) dx$$

where: $p=0, 1, 2, 3 \dots$

$$-\frac{lC_0}{p\pi} \cos\left(\frac{p\pi x}{l}\right) \Big|_0^l = \left\{ (0 \text{ if } m \neq p); \left(\frac{A_m l}{2} \text{ if } m = p\right) \right\}$$

\therefore for $m = p = 1, 3, 5 \dots$

$$\frac{2lC_0}{m\pi} = \frac{A_m l}{2}$$

$$A_m = \frac{4C_0}{m\pi}$$

Finally, the solution to the diffusion equation for a solute of constant concentration diffusing into a slab becomes:

$$C(x, t) = \frac{4C_0}{\pi} \sum_{n=0}^{\infty} \frac{1}{2n+1} \sin\left(\frac{(2n+1)\pi x}{l}\right) \exp\left(-\frac{D(2n+1)^2\pi^2}{l^2} t\right)$$

where the slab is bounded by $x = 0$ and $x = l$. In the present case, the solid is symmetric if the origin ($x = 0$) is placed along the mid-plane in the sample and the diffusion length l is taken to be half the thickness of the coupon. The solution to the diffusion equation becomes:

$$C(x, t) = \frac{4C_0}{\pi} \sum_{n=0}^{\infty} \frac{1}{2n+1} \sin\left(\frac{(2n+1)\pi x}{2l}\right) \exp\left(-\frac{D(2n+1)^2\pi^2}{4l^2} t\right)$$

The flux of tritium ($F(t)$) approaching and then leaving the surface of the coupon at $x = l/2$ is:

$$F(t) = -D \frac{\partial c}{\partial x} \quad \text{evaluated at } x = l/2$$

$$= -D \left[-\frac{4C_0}{\pi} * \frac{\pi}{2l} * \sum_{n=0}^{\infty} \cos\left(\frac{(2n+1)\pi x}{2l}\right) \exp\left(-\frac{D(2n+1)^2\pi^2}{4l^2} t\right) \right]$$

$$F(t) = \frac{2C_0D}{l} \sum_{n=0}^{\infty} \exp\left(-\frac{D(2n+1)^2\pi^2}{4l^2}t\right)$$

and the rate at which tritons leave the coupon of surface area (A) at $x = l/2$, will be

$$\dot{n}_s = A * F(t) = \alpha * e^{-t/\tau} \quad (1)$$

where:

$$\tau = \frac{4l^2}{D\pi^2} \quad (2)$$

and

$$\alpha = \frac{2c_0DA}{l} \quad (3)$$

In the limit of long times, $n=0$, the summation can be dropped.

Tritons released from the metal surface are swept from the decontamination chamber volume (V) at a flow rate (F). The rate at which tritium particles leave the chamber depends on the number of particles in the chamber, the carrier flow rate, and the chamber volume according to the relation:

$$\dot{n}_f = \frac{F}{V} * N(t) = \beta N(t) \quad (4)$$

where $N(t)$ is the number of tritons in the chamber at time t .

The number of tritons in the chamber at any time, t , equals the number released from the metal surface minus those swept away by the carrier:

$$\frac{dN}{dt} = \dot{n}_s - \dot{n}_f$$

or using equations 1 and 4:

$$\frac{dN}{dt} = \alpha e^{-t/\tau} - \beta N \quad (5)$$

The method of using an Integrating Factor can be used to solve the mass balance equation (equation 5). Multiplying equation 5 by $e^{\beta t}$ and separating the variables yields:

$$e^{\beta t} \frac{dN}{dt} + \beta N e^{\beta t} = \alpha e^{(\beta - \frac{1}{\tau})t}$$

Integration yields:

$$N e^{\beta t} = \alpha \left(\frac{1}{\beta - \frac{1}{\tau}} \right) e^{-\frac{t}{\tau}} * e^{\beta t} + C$$

or

$$N(t) = \gamma e^{-\frac{t}{\tau}} + C e^{-\beta t} \quad (6)$$

where:

$$\gamma = \frac{\alpha \tau}{\beta \tau - 1} \quad (7)$$

and C is a constant of integration.

At the start of the experiment ($t = 0$), the number of tritons in the carrier $N(0) = N_0$, the background value. Applying this condition to equation 6 shows that the constant of integration is:

$$C = (N_0 - \gamma)$$

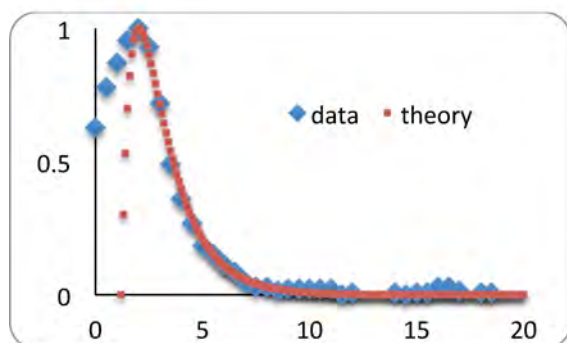
and equation 6, the number of tritons swept from the chamber at any time, t, becomes:

$$N(t) = \gamma e^{-\frac{t}{\tau}} + (N_0 - \gamma) e^{-\beta t} \quad (8)$$

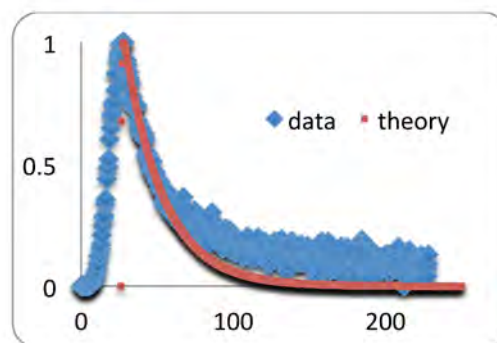
where all the parameters are known except for the diffusion coefficient. Since the source of the tritons is the metal surface, equation 8 multiplied by the carrier flow rate, divided by the chamber volume and the surface area of the coupon represents the rate at which tritons desorb from the metal surface per unit time and area, i.e. the outgassing rate.

Results and Discussion

Equation 8 was fit to the data by varying the diffusion coefficient until the best fit to the experimental data was obtained. These fits are shown in Figure 3 for the different outgassing temperatures. The experimental data shown in these figures was obtained by differentiating the amount of activity collected in bubbler (B1) with respect to time and by dividing the result by the surface area of the coupons. Each data set shows the same basic structure of a quick rise in the outgassing rate followed by a slow decay in the outgassing rate. Seven cases are shown: in each of these cases, the furnace was brought to a specific temperature within 3 minutes and subsequently held at that temperature for the remainder of the experiment. The coupons could take up to 20 minutes to reach the target temperature. Both the data and the theoretical fits in these figures were normalized to their respective maximum values. The model has two major shortcomings: it does not fit the data very well at both short and long times except for the 20 and 400°C cases. This suggests that at these temperatures, the outgassing rate is dominated by a single diffusion coefficient. At 20°C, desorption may be restricted by tritium diffusion and desorption from the surface oxide layer. On the other hand, at 400°C, tritium diffusion through the metal may be the rate-limiting step. At the intermediate temperatures, at least two processes are involved in the transfer of tritium from the bulk to the carrier stream resulting in a poor curve fit when modeled by a single adjustable parameter.



20°C



100°C

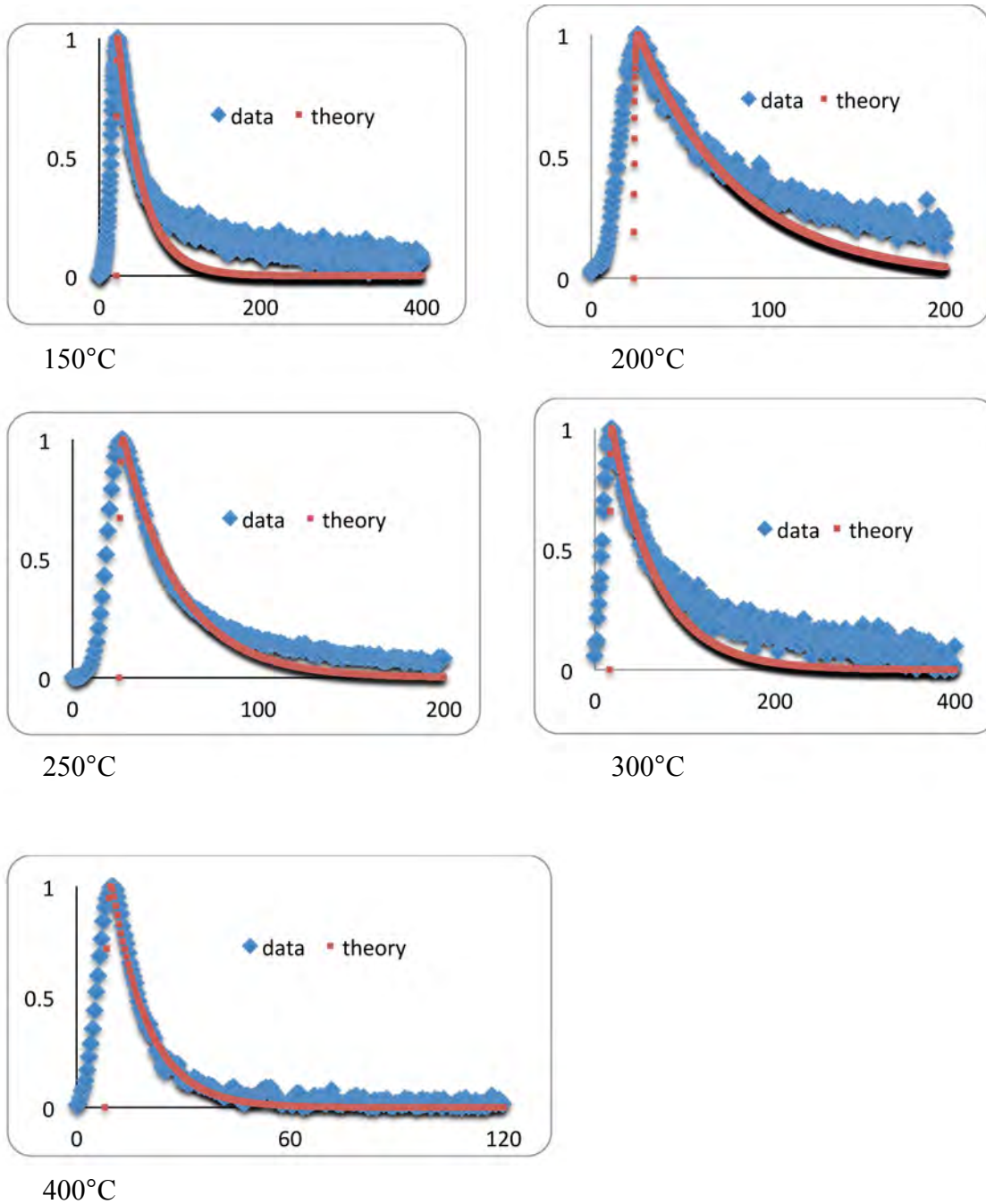


Figure 3 Comparison of normalized predicted outgassing rate with normalized experimental data against time in minutes for different coupon temperatures

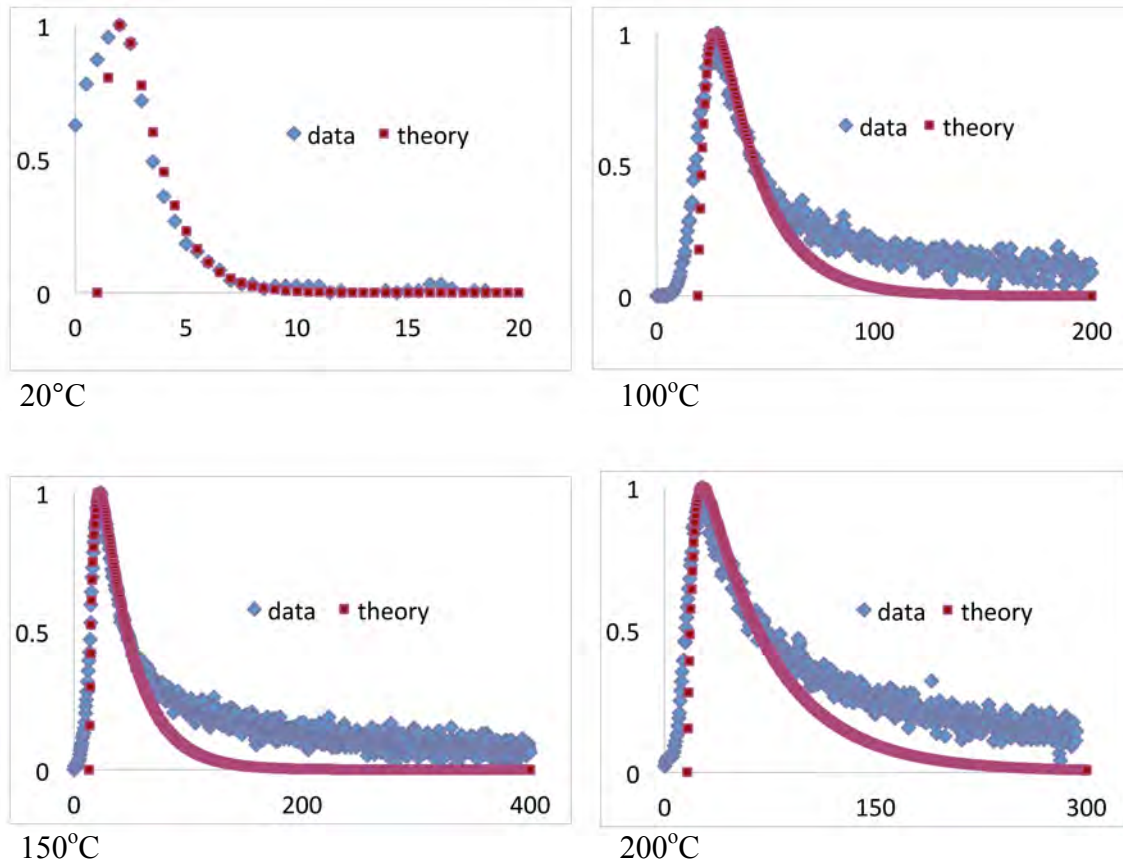
The model described above assumes the diffusion coefficient to be constant, fixed at the final desorption temperature for the duration of the experiment. In reality however,

tritium was released from the metal surface during the first 30 minutes of the experiment while the coupon was heating up to its final temperature. The diffusion coefficient, which has the following Arrhenius dependence on temperature:

$$D(T) = D_o \exp\left(-\frac{E_a}{RT}\right)$$

where D_o is the diffusion coefficient (cm^2/s), E_a is the activation energy for diffusion (kJ/mol), and R is the gas constant ($8.314 \text{ J/mol}\cdot\text{K}$), increases as the sample is heated up to its final temperature. Consequently the time constant τ specified in equation 2 and γ by equation 7 modify equation 8.

Figure 4 compares the normalized predicted outgassing rate with experimental data against time for the different coupon temperatures taking into account the changing diffusivity during the first 30 minutes.



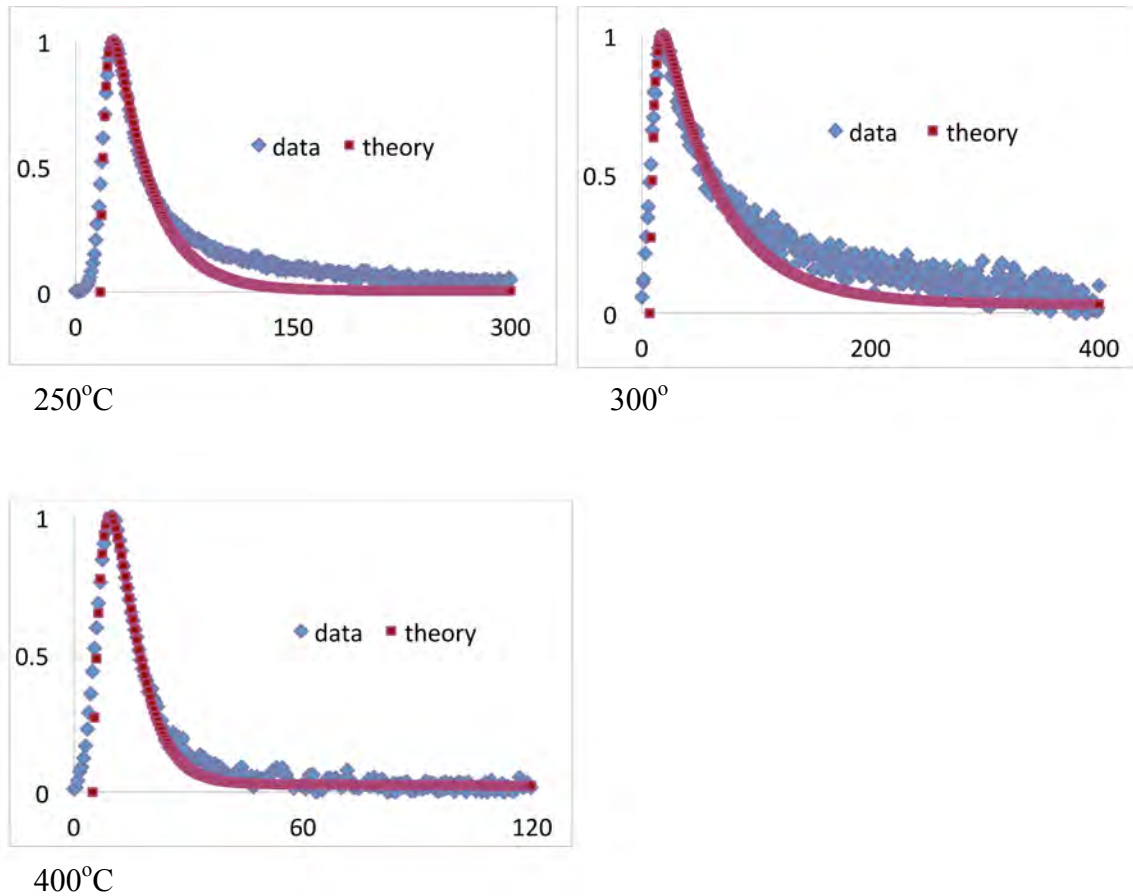


Figure 4: Comparison of normalized predicted outgassing rate with normalized experimental data against time in minutes for different coupon temperatures and accounting for the temperature dependence of the diffusivity.

As expected the fit between normalized prediction and experimental data improves noticeably during the first hour of each run in which the temperature is ramped above room temperature. The fit at longer times remains poor for the intermediate temperatures.

Figure 5 compares the diffusion coefficients calculated from the fits at each temperature to data published by Austin [8] and Tanabe [9, 10] for diffusion of tritium through bulk stainless steel (type 316). With the possible exception of the two data points at the highest temperatures investigated in this study, 300°C and 400°C, the magnitude and trend of the inferred diffusivities do not agree with literature values. The diffusivities

inferred from the tritium release at temperatures below 300°C do not follow the expected temperature behavior. The surface oxide must play an important role in restricting tritium mobility from the bulk to the air/metal interface. The decay time in equation 8 depends on both τ and β , the former dependent on the l^2/D ratio and the latter on the purge rate through the decontamination chamber. If the purge rate remains fixed, the decay time in equation 8 will remain unchanged if the l^2/D ratio remains unchanged. If the diffusivity through the oxide layer dominates hydrogen transport and is assumed to be of the same order of magnitude as for stainless steel, then the oxide layer must be approximately 0.1 μm at room temperature. Stainless steel typically has between 100 and 300 monolayers on its surface. Since each monolayer is approximately 0.3 nm thick, typical oxide thicknesses on stainless steel range from 0.03 μm to 0.1 μm in line with the estimate given above. The transport of hydrogen from the bulk through the oxide into the carrier must depend on the diffusivity through bulk metal and metal oxide in the temperature range 20°C and 300°C.

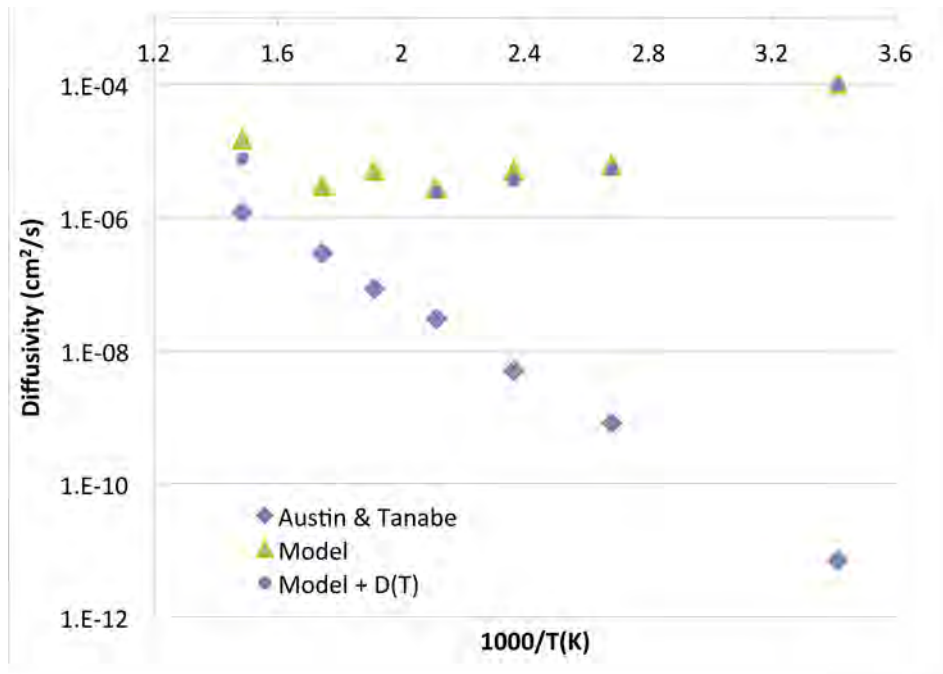


Figure 5. Plot of the tritium diffusion coefficient dependence on temperature of stainless steel

Summary and Future Work

A simple model has been developed to describe the outgassing rate of tritium from a finite solid as a function of time. The model is based on the assumption that hydrogen transport through a homogeneous substrate can be characterized with a single diffusion coefficient. The model was used to fit experimental tritium desorption rates of tritiated type 316 stainless steel over a temperature range of 20 to 400°C. The model reproduces general features of the outgassing data. However, the diffusion coefficients inferred from the fitted curves do not agree with published data although the inferred values approach published values at the highest temperatures investigated. Additionally the model cannot accurately predict the experimental data over the entire desorption profile suggesting that the model using a single fit parameter cannot describe the processes of tritium desorption from stainless steel with an oxide layer.

A more comprehensive model is needed to describe tritium release accurately. This model should include three components:

- 1) desorption from the surface of the oxide layer,
- 2) diffusion through the oxide layer, and
- 3) diffusion through the bulk.

References

1. San Marchi, C.; Somerday, B. P.; Robinson, S. L. Permeability, Solubility and Diffusivity of Hydrogen Isotopes in Stainless Steels at High Gas Pressure. *Inter. J. Hydrogen Energy*, 32, 100-116 (2007).
2. Causey, R. A., Karnesky, R. A., & San Marchi, C. (2011). "Tritium Barriers and Tritium Diffusion in Fusion Reactors". In R. J. M. Konings, & R. E. Stoller (Eds.), *Comprehensive Nuclear Materials* (Chapter 116). Elsevier. ISBN: 008056027X.
3. Antoniazzi, A.B., Shmayda, W.T., Surette, R.A., *Fusion Technol*, 21, 867, (1992)
4. Shmayda, W.T., Antoniazzi, A.B., Surette, R.A., Ontario Hydro Research Division, Report # 92-51-K, (1992)
5. Carslaw, H.S.; Jaeger, J.C.; *Conduction of Heat in Solids 2nd Ed.*, Clarendon Press: Oxford, England, 1959, p. 93
6. Penzhorn, R.-D.; Torikai, Y.; Naoe, S.; Akaishi, K.; Perevezentsev, A.; Watanabe, K.; Matsuyama, M., *Fusion Sci. Tech.* 57, 185 (2010).
7. Hollenberg, G.W.; Simonen, E.P.; Kalinin, G., *Fusion Eng. Design*, 28, 190 (1995).
8. Takeishi, T.; Nishikawa, M.; Katayama, K. *Fusion Eng. Design*, 61-62, 591 (2002).
9. Postolache, C.; Matei, L. *Fusion Sci. Tech.*, 48, 413 (2005).

10. Carslaw, H.S.; Jaeger, J.C. *Conduction of Heat in Solids*, 2nd Ed. Clarendon Press, Oxford, England. 1986. p. 93 – 96
11. Austin, J. H.; Elleman, T.S., *J. Nuc. Mater.*, 43, 119 (1972).
12. Tanabe, T.; Yamanishi, Y.; Sawasa, K.; Impto, S.; *J. Nuc. Mater.* 122 & 123, 1568 (1984).
13. Tanabe, T. *Fusion Eng. Design*, 10, 325 (1989).